Binding Energy of $F(H_2O)^-$ and the Simulation of Fluoride Water Clusters Using a Hybrid QM/MM (Fluctuating Charge) Potential

Richard A. Bryce, Mark A. Vincent, and Ian H. Hillier*

Department of Chemistry, University of Manchester, Manchester M13 9PL, U.K.

Received: January 7, 1999; In Final Form: March 17, 1999

High-level ab initio calculations have been used to determine the binding energy of $F(H_2O)^-$. A value of −27.3 kcal/mol has been obtained, which is considerably greater than the experimental value near −23 kcal/mol. The new theoretical value is used to parametrize a hybrid quantum mechanical (QM)/molecular mechanical (MM) potential in which F^- is described at a high level of quantum mechanics and H_2O is modeled with a fluctuating charge MM potential. Static and dynamic calculations of $F(H_2O)_4^-$ are carried out using this hybrid QM/MM potential. Static calculations using both full electronic structure methods and the hybrid potential predict a range of interior and surface structures within 2 kcal/mol, while molecular dynamics simulation at 300 K using the hybrid potential suggests that a range of structures will be observed.

1. Introduction

Recent advances in spectroscopic techniques, coupled with high-level quantum chemical calculations, have yielded detailed insight into the dynamical and energetic behavior of small water clusters, ranging from dimers to octamers.[1−4] The potential energy surface derived from detailed theoretical studies is complex in form and the dynamical behavior of the water molecules highly cooperative. To further advance our understanding of intermolecular forces, it is desirable to examine the properties of small water clusters in the presence of strong electric fields, as encountered in the hydration of ions.

The subject of considerable interest and indeed some controversy has been the structural behavior of small water clusters containing halide anions. Two principal configurations have been observed from simulation studies: the anion residing principally at the surface of the cluster (s state), and mainly in a solvated, interior state (i state). With successive addition of water molecules to the cluster, a surface to interior transition has been found to occur for all the halide monoanions. Contradictory results have been found from theoretical investigations of fluoride/water clusters,[5−9] aggravated by uncertainty in experimental measurements and difficulty in accurately modeling the unusually strong fluoride/water−hydrogen interaction, even at high levels of electronic structure theory. Through the application of mass spectroscopy, incremental enthalpies of association were measured by Ashadi et al.[10] for $F(H_2O)_n^-$ clusters over the range $n = 1-5$, finding the enthalpy of binding of a single water to a fluoride anion to be −23.3 kcal/mol. Simulation studies using a dipole polarizable water model fitted to this experimental result found the s → i transition to occur upon addition of the fourth[6] water molecule, considerably earlier than for larger halides. However, more recent experimental studies of F^- solvated by 2−10 water molecules by Hiraoka et al.,[11] also using high-pressure mass spectroscopic techniques, found incremental enthalpies 3−15% larger than in Ashadi's study. In agreement with these later experimental findings, subsequent high-level ab initio calculations at the MP2/aug-cc-pVXZ (X = D,T) level of theory[12] found fluoride/water binding energies about 20% greater than the $n = 1-3$ experimental measurements.[10] Simulations[9] using a potential refitted to the greater ab initio binding enthalpy of −26.5 kcal/mol observed the s → i transition upon the addition of the sixth water molecule, earlier than in a previous study.[8]

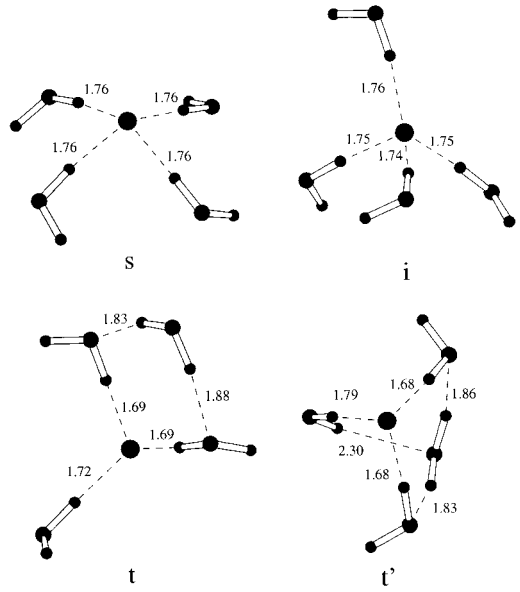

Figure 1. Structures of (s) surface, (i) interior, and (t,t′) trisolvated states of $F(H_2O)_4^-$ at QM/MM(FQ) optimized geometry. Bond lengths in Å.

Second solvation shell effects have found to be important,[12] as observed in a study of the $n = 4$ cluster by us,[13] employing a fluctuating charge (FQ) model of the solvent after the method of Rick et al.,[14] in combination with a quantal description of the fluoride anion. Thus, a fully polarizable representation of the system was facilitated under this hybrid quantum mechanical (QM)/molecular mechanical (MM) potential, denoted QM/MM-(FQ). With the intersolvent and solute−solvent interactions fitted to experiment, a trisolvate configuration (t state, Figure 1) with only three direct H···F hydrogen bonds was observed to be the lowest in energy at 0 K, lower indeed than the s and i states (Figure 1). Simulations at room temperature also found this t state to be the most populated. A thorough exploration of second solvation shell effects using ab initio and density functional

10.1021/jp9900990 CCC: $18.00
Published on Web 04/30/1999

methods confirmed that a trisolvate state was indeed the lowest in energy.[15] However, a Monte Carlo simulation[15] using a fully quantum mechanical potential (MP2/6-311++G(3d,2p)) observed that at 300 K, interior, solvated states dominated, with only trace amounts of trisolvate configurations, in direct contrast to the QM/MM(FQ) study. It must be noted, however, that in the QM/MM(FQ) model, the fluoride/water interaction energy was parametrized using the binding energy of Ashadi et al. Furthermore, recent very high level calculations of the water dimer have suggested that the experimentally determined interaction energy has been overestimated.[16−20] In light of mounting evidence indicating overestimation of the intersolvent and underestimation of the ion−solvent interactions, we reappraise our parametrization of the QM/MM(FQ) potential, presenting a new ab initio study of the fluoride/water interaction, estimated up to the QCISD(T,FULL)/aug-cc-pV5Z level of theory. Subsequent energetic and dynamical results using the hybrid potential are presented. We focus on the fluoride ion solvated by four water molecules, since a cluster of this size shows a range of different structures that are quite close in energy.[13,15]

2. Computational Details

2.1. Electronic Structure Calculations. Any approach to study the hydrogen bond strength of $F(H_2O)^-$ must be able to describe the fluoride ion and water molecule correctly. Thus, we have chosen the aug-cc-pVXZ (X = T, Q, and 5) basis sets of Dunning[21,22] as they are designed for anions and are large and flexible. Levels of theory used with these basis sets are second-order Moller−Plesset perturbation theory (MP2),[23] quadratic configuration interaction with single and double substitutions (QCISD),[24] QCISD with triples contribution to the energy (QCISD(T)),[24] and the density functional theory using the B3LYP functional.[25] Geometries and frequencies have been determined by analytical methods for all B3LYP results, for the MP2 results (aug-cc-pVTZ and aug-cc-pVQZ basis sets only) and for the QCISD results. Optimal geometries at the MP2 level with the aug-cc-pV5Z basis set and geometries and frequencies at the QCISD(T) level were determined via fitting the calculated energies to a polynomial in the bond lengths and angles. There may be an inconsistency between B3LYP and MP2 calculations, in that B3LYP describes the entire electron density and MP2 often correlates only the valence electrons. To see the effect of the core electron correlation at the MP2 and QCISD(T) levels, $F(H_2O)^-$ calculations were carried out involving the 1s electrons of oxygen and fluorine. These calculations are distinguished from those including only valence electron correlation by being designated FULL. The contribution of basis set superposition error to the binding energy of $F(H_2O)^-$ was also investigated. For consistency with our previous study[15] of the solvation of F^- we have used six d-functions. Calculations used the GAUSSIAN 94 suite of programs,[26] including our implementation of the distributed multipole analysis (DMA) after the method of Stone.[27]

2.2. Polarizable Potential. A hybrid QM/MM potential is employed,[28] recently extended by us to incorporate a fluctuating charge classical region.[29] Here, the fluoride anion is treated quantum mechanically and the surrounding aqueous environment via a force field representation, using the FQ implementation of the simple point charge (SPC) water model.[14] The FQ water model allows charge to flow between sites within each molecule, such that the instantaneous atomic electronegativities are equalized. The charge flow within the classical waters is influenced by atomic electronegativity parameters and by Coulombic interactions. This electrostatic interaction involves an intramolecular component, where screening is incorporated, and an intermolecular component with other FQ waters and with the electrons and nuclei of the QM region. Electronegativities and screening parameters were taken from the work of Rick et al.[14] We have implemented this QM/MM(FQ) potential using the QM/MM program described earlier[28] utilizing GAUSSIAN 94.[26]

2.3. Simulation Method. To simulate the motion of fluoride/water clusters using the QM/MM(FQ) potential, it is necessary to employ an extended Lagrangian for the system, which incorporates both the dynamics of the translational coordinates and of the atomic partial charges. Consequently, a fictitious kinetic energy for the charges is incorporated, involving a charge mass, M_Q. It is important to ensure that an adiabatic separation is maintained between the two dynamical subsystems. To obviate heat transfer between the regimes, the fictitious charge mass can be adjusted. Previous studies indicate that a mass of 6.9×10^{-5} (ps/e)^2 kcal/mol is appropriate.[13] Additionally, one can directly thermostat the temperature of the subsystems to prevent equilibration. Two simulations were performed for the $F(H_2O)_4^-$ cluster, both of 50 ps duration in which the equations of motion were solved using the standard velocity Verlet algorithm[30] with a time step of 1 fs and RATTLE[31] to maintain the SPC internal geometry of the water molecules. The final 30 ps were used for analysis. The first trajectory was followed within the microcanonical ensemble, starting from the optimized interior structure, where for the duration of the simulation the temperature of the charges was observed not to exceed 1 K. A second simulation was performed within the canonical ensemble at a temperature of 300 K, to afford a more direct comparison with the experimental studies conducted at room temperature. Separate Nosé−Hoover thermostats[32,33] were employed for the translational and charge degrees of freedom: the atomic motion was maintained at 300 K using a thermostat mass of 10^4 au; charge dynamics were performed at 2 K using a thermostat mass of 10^3 au. The simulation was initiated from the optimized surface structure. To analyze the geometry of the cluster along the simulated trajectories, an order parameter, Q, was used, given by

$$Q = {}^1/_4\langle|\hat{\mathbf{r}}_{12}\cdot\hat{\mathbf{r}}_{13}\times\hat{\mathbf{r}}_{14}| + |\hat{\mathbf{r}}_{21}\cdot\hat{\mathbf{r}}_{23}\times\hat{\mathbf{r}}_{24}| + |\hat{\mathbf{r}}_{31}\cdot\hat{\mathbf{r}}_{32}\times\hat{\mathbf{r}}_{34}| + |\hat{\mathbf{r}}_{41}\cdot\hat{\mathbf{r}}_{42}\times\hat{\mathbf{r}}_{43}|\rangle \quad (1)$$

where $\mathbf{r}_{ij}$ is a unit vector joining oxygen atoms i and j. For a pyramidal structure, $Q = 0$, whereas for a tetrahedron, $Q = 0.73$. We can then calculate the probability density, $P(Q)$, of finding a configuration with an order parameter Q. Binding enthalpies were calculated from the simulations using the relation,

$$\Delta H = \langle\Delta U\rangle - \Delta nRT \quad (2)$$

where Δn is the difference in the number of species upon binding (i.e., 4 molecules), and ΔU is the total energy of the system.

3. Results

3.1. Electronic Structure. It is imperative that any methods used for studying $F(H_2O)^-$ be able to accurately describe the two isolated components of the dimer. To this end we carried out a set of calibration calculations on the ionization energy of F^- and the structure and vibrational frequencies of H_2O. The results are tabulated in the Supporting Information. In summary,

TABLE 1: Geometry (Å, deg) of the Complex $F(H_2O)^-$ [a]

	F···H	H−O	O−H′	F···H−O	H−O−H′
B3LYP/aug-cc-pVTZ	1.390	1.062	0.960	177.1	102.8
B3LYP/aug-cc-pVQZ	1.391	1.061	0.959	177.0	102.9
B3LYP/aug-cc-pV5Z	1.391	1.060	0.959	177.0	102.9
MP2/aug-cc-pVTZ	1.373	1.064	0.960	177.6	101.9
MP2(FULL)/aug-cc-pVTZ	1.376	1.059	0.958	177.5	102.0
MP2/aug-cc-pVQZ	1.375	1.061	0.957	177.3	102.0
MP2(FULL)/aug-cc-pVQZ	1.366	1.062	0.956	177.5	102.1
MP2/aug-cc-pV5Z	1.380	1.059	0.957	177.2	102.0
QCISD/aug-cc-pVTZ	1.403	1.044	0.958	176.8	102.1
QCISD(T)/aug-cc-pVTZ	1.387	1.055	0.961	177.1	101.9
QCISD(T,FULL)/aug-cc-pVTZ	1.391	1.050	0.959	177.0	102.0

[a] For all structures F···H−O−H′ is 0.0°.

TABLE 2: Calculated Vibrational Frequencies (cm^{-1}) of $F(H_2O)^-$

	aug-cc-pVTZ			aug-cc-pVQZ
	B3LYP	MP2[a]	QCISD(T)[b]	B3LYP
stretch of F^-···H	390	394 (395)	383 (377)	386
in-plane rotation of H_2O	577	587 (604)	583 (598)	573
out-of-plane vibration of H	1154	1195 (1251)	1145 (1239)	1143
bend of H−O−H′	1691	1706 (1725)	1728 (1742)	1690
stretch of H−O	2153	2124 (2169)	2209 (2241)	2155
stretch of O−H′	3850	3890 (3902)	3855 (3841)	3857

[a] MP2(FULL) values in parentheses. [b] QCISD(T,FULL) values in parentheses.

they show that the B3LYP results are essentially converged to the basis set limit for all properties considered with the aug-cc-pVTZ basis set, though the ionization energy of F^- is overestimated by about 0.1 eV.

We turn now to our calculation of the $F(H_2O)^-$ complex, summarized in Tables 1 and 2. The optimal structures (Table 1) again demonstrate convergence of the density functional method with increasing basis set size. For the MP2 (valence only correlation) wave function the geometrical parameters are converging as the basis set is increased with the exception of the H···F length. The change in this value is greater from the quadruple-ζ basis to the pentuple-zeta basis (1.375 to 1.380 Å) than from the triple-ζ to quadruple-ζ (1.373 to 1.375 Å). However, we note that this length is highly coupled to the H−O length, which shows a slower convergence to a limit than does the other O−H′ bond length. Here hydrogen atom H, rather than H′, is hydrogen bonded to F^-. This odd structural behavior is again shown by the MP2(FULL) results, where the trend in bond lengths in going from the aug-cc-pVTZ to the aug-cc-pVQZ is reversed from the valence only result (1.376 to 1.366 Å). Thus, estimation of the geometry at the MP2 limit is difficult. On top of this there are modest changes in geometry when higher order correlation effects are included via the QCISD(T) method. Thus the H···F bond length increases by 0.014 Å and the H−O bond length decreases by 0.009 Å comparing MP2 and QCISD(T) (aug-cc-pVTZ) values. For the geometries given by the QCISD(T,FULL) method compared to those given by the MP2(FULL) method, equally large changes are observed (0.015 and 0.009 Å). Comparing the QCISD(T) and QCISD(T,FULL) (aug-cc-pVTZ) geometries (Table 1), the angles are very similar and the bond lengths vary by up to 0.005 Å. From the geometrical data in Table 1, we cannot be certain that the geometrical parameters have reached their basis set limit at the MP2 level with the aug-cc-pV5Z basis (valence only correlation), in contrast to the B3LYP results.

For the aug-cc-pVTZ basis set there are no great differences in the calculated vibrational frequencies (Table 2) among the different correlation methods, though two modes do show a range of values of over 100 cm^{-1}. There are perhaps two surprising things about this set of frequencies. First, the quite short H···F bond has a low vibrational frequency at 377−395 cm^{-1}. Second, the out-of-plane mode is not a low-frequency one but occurs at 1143−1251 cm^{-1}. It might be expected that the H′ atom would rotate about the pseudolinear F···H−O axis giving a low-energy internal rotation mode, but in fact it is the other hydrogen that vibrates out of plane. This can perhaps be best explained as the F···H−O behaving as a linear system and the mode being a perturbed linear bend. The vibrational frequencies have been studied before by Yates et al.,[34] whose values are 4044, 2670, 1789, 1125, 562, and 346 cm^{-1}. Their O−H′ mode is some 140−200 cm^{-1} larger than ours, but a little more surprising is that the other H−O mode is different from our values (2124−2241 cm^{-1}) by at least 400 cm^{-1}. This difference appears to be due to methodology rather than basis sets (CISD versus MP2, QCISD(T), and B3LYP). Yates et al.[34] do give a set of anharmonic corrections for their frequencies which we can apply to our modes to give a set of predicted experimental frequencies. However, since we are not at the basis set limit for geometry, frequencies may vary with geometry change. If we take our QCISD(T,FULL) frequencies and apply Yates et al.'s corrections, we obtain values of 3664 (O−H′ stretch) 1678 (H−O−H bend), 1606 (H−O stretch), 1258 (out-of-plane F···H−O bend), 598 (in plane rotation of water), and 371 (F···H stretch) cm^{-1}. We note that the large anharmonic shift of the order of 630 cm^{-1} for the H−O mode has also been determined by Janoschek.[35]

The predicted binding energies of $F(H_2O)^-$ are shown in Table 3. For the B3LYP wave function, the results converge to a value close to −27.0 kcal/mol. Considering both the counterpoise corrected results (MP2/CP) and the uncorrected results (MP2) in Table 3, they seem to be converging to a common value near −27.1 kcal/mol. These results are consistent with those of Xantheas.[20] The QCISD(T)/aug-cc-pVTZ results indicate a higher order correlation correction of about 0.2 kcal/mol (compared to the MP2 value), giving a binding energy at 0 K of −27.3 kcal/mol. A similar argument applied to the MP2 values including core electron correlation also gives a basis set limit binding energy of −27.1 kcal/mol, which increases to −27.3 kcal/mol when corrected for higher order correlation effects. Thus, this is our final estimate of the interaction energy

TABLE 3: Binding Energy of $F(H_2O)^-$ (kcal/mol)

	basis set aug-cc-pVXZ		
	X = T	X = Q	X = 5
B3LYP	−27.3	−27.1	−27.0
MP2	−27.7	−27.4	−27.3
MP2/CP	−26.5	−26.7	−26.9
MP2(FULL)	−28.1	−27.7	
MP2(FULL)/CP	−26.4	−26.7	
QCISD(T)[a]	−27.9 (−28.3)		

[a] The number in parentheses is the binding energy including correlating all core and valence electrons.

TABLE 4: Interaction Energy of Water Dimer

model	ΔE (kcal/mol)	R_∞ (Å)	ref
MP2	−5.0	2.925	17
QM/MM(FQ)	−5.0	2.804	this work
experiment	-5.4 ± 0.2	2.98	38, 39

at 0 K. We use this value of −27.3 kcal/mol to reparametrize the fluoride−water interaction potential.

To obtain an enthalpy of interaction to compare to experiment, we first include zero-point effects giving a value of $\Delta H^{0\,K}$ of −26.4 kcal/mol (QCISD(T,FULL)/aug-cc-pVTZ), which is modified to −26.6 kcal/mol when anharmonicity is included in the modes for the complex and water. Further correction for finite temperature effects gives ($\Delta H^{298\,K}$) to be −27.7 kcal/mol, a value significantly greater than the experimental value of about −23 kcal/mol and Combariza and Kestner's value of 24.5 kcal/mol.[36]

Having obtained a reliable estimate of the fluoride/water interaction energy, we turn now to consider the magnitude of the intersolvent hydrogen bond. Molecular beam experiments[37] have found the geometry of the water dimer to be of C_s symmetry. Experiment[38] has also shown the interaction energy, corrected for finite temperature and vibrational effects, to be -5.4 ± 0.7 kcal/mol, confirmed by a subsequent study[39] with narrower error bars of 0.2 kcal/mol. This hydrogen bond strength is naturally much smaller than that of the fluoride−water bond, due to the charged nature of the fluoride species. However, as with theoretical studies on the $F(H_2O)^-$ system, ab initio studies have been at variance both with experiment and with other ab initio studies. Recent calculations[16−20] have clustered around the lower region of the experimental value. The water dimer interaction energy at the Hartree−Fock limit has been calculated[17] as −3.64 kcal/mol, implying the significance of correlation effects. Furthermore, correction for basis set superposition error, including fragment relaxation, has been shown to be important.[20] The most comprehensive calculation to date has been a frozen core MP2 calculation by Schütz et al.,[17] using an atomic natural orbital (ANO)-type basis set (1046 basis functions), leading to an estimated interaction energy of −4.9 kcal/mol. From this result, they incorporated the effects of core/core and core/valence correlation (−0.04 kcal/mol), method truncation (−0.06 kcal/mol), and fragment relaxation in the counterpoise correction (0.02 kcal/mol). This leads to a complete basis set estimate of -4.98 ± 0.05 kcal/mol (Table 4), which was taken to be the basis for parametrization of the QM/MM-(FQ) water−water interaction.

3.2. Cluster Potential. Based upon our results for $F(H_2O)^-$ and the previously discussed results for $(H_2O)_2$, our QM/MM-(FQ) model was reparametrized.[13] We first consider the water−water potential. The energy of interaction between two classical fluctuating charge waters was fitted by adjustment of the oxygen Lennard-Jones parameters (Table 5) to yield the value obtained by Schütz of −4.98 kcal/mol. The resulting interoxygen distance

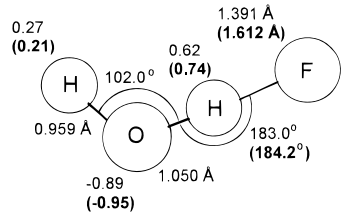

Figure 2. Optimized geometries for $F(H_2O)^-$: comparison of QCISD-(T,FULL)/aug-cc-pVTZ and QM/MM(FQ) (bold, parentheses) models. Comparison of QM/MM(FQ) (bold, parentheses) charges (in e) with Mulliken analysis of MP2(FULL)/aug-cc-pVQZ wave function.

TABLE 5: Lennard-Jones Parameters for QM/MM(FQ) Model

atom type	σ (Å)	ϵ (kcal/mol)
O	3.188	0.1823
F^-	2.988	0.7550

at the minimum of the FQ potential was 2.804 Å (Table 4), 0.2 Å shorter than the experimentally observed value. Insight into the polarization of water effected by dimerization may be obtained by consideration of a recent charge distribution analysis by Åstrand et al.,[40] employing atomic polar tensor-based (APT) partial charges. We adopt their notation, referring to the bonding proton of the water hydrogen bond donor as H_{db} and the protons of the accepting water as H_a. Using large ANO basis sets, APT analysis of an isolated water molecule at the experimental geometry yields a charge of 0.28 e on the hydrogens, slightly smaller than the fluctuating charge value of 0.34 e. However, in the dimer complex, both APT and fluctuating charge calculations predict an increase of 30−40% in the magnitude of H_{db}, with values of 0.39 and 0.45 e, respectively. The charge separation within both APT and FQ donor waters is identical, with a difference of 0.14 e between protons. Compared to H_{db}, the H_a protons in the hydrogen bond accepting water are more mildly polarized, having a charge of 0.39 e within the FQ model, compared to about 0.31 in the APT acceptor. We may therefore conclude that the FQ model provides a reasonable microscopic model of solvent polarization.

Turning now to the water−fluoride interaction, the van der Waals parameters of a fluoride ion described quantum mechanically, interacting with a classical fluctuating charge water, were fitted to obtain a QM/MM interaction energy of −27.3 kcal/mol, in accord with our most accurate estimate from ab initio calculations (section 3.1). The fluoride was described at the B3LYP level with a 6-311++G(3d,2p) basis set. This model was derived from an ab initio study with the 6-31+G* and 6-31G* basis sets, considering the interior/surface energy difference and comparing a number of methods to QCISD(T).[15] Although MP2 essentially reproduced the QCISD(T) result, the B3LYP calculation only differed by 0.2 kcal/mol. In light of this and the less computationally expensive gradients required for dynamical studies, the B3LYP density functional was adopted. Basis set effects were then explored in relation to the MP2/aug-cc-pVTZ calculation on $F(H_2O)^-$, and the valence triple-ζ 6-311++G(3d,2p) basis set of functions was adopted.

The geometry of $F(H_2O)^-$ calculated by the QM/MM(FQ) method with the derived Lennard-Jones parameters of the fluoride (Table 5) is compared to the QCISD(T,FULL)/aug-cc-pVTZ geometry in Figure 2. In contrast to the water dimer, the QM/MM(FQ) model overestimates the intermolecular distance, with a H···F length of 1.612 Å compared to an MP2 value of 1.391 Å. This is not too unexpected in the light of the low frequency associated with the H···F stretching motion (Table 2). However, the linearity of the H···F bond is faithfully

TABLE 6: Interaction Energies of $F(H_2O)_4^-$ Clusters (kcal/mol) at Various Levels of Theory

state	QM/MM(FQ)	B3LYP[a]	MP2[a]
i	−78.3	−81.5	−82.6
s	−77.4	−80.5	−82.4
t	−78.6	−82.1	
t′	−77.8	−82.7	−84.0

[a] Reference 15.

reproduced, as too is the extent of the polarization, as illustrated by the agreement to within 0.12 e, between the QM/MM(FQ) partial charges and those derived from a Mulliken analysis of the MP2(FULL)/aug-cc-pVQZ wave function. Interestingly, here we find a Mulliken charge of −1.0 e on the anion, indicating little charge transfer.

We may then apply this revised polarizable solute/solvent potential to the study of the $n = 4$ fluoride/water clusters. The recent MP2/6-311++G(3d,2p) study of $F(H_2O)_4^-$ by Vaughn *et al.*[15] identified at least seven stationary points within 5 kcal/mol of the lowest energy minimum. Of these eight structures, one was disolvate, five were trisolvate, and two tetrasolvate (the interior and surface configurations). The global minimum is denoted state t′ and is shown in Figure 1. Interestingly, however, the t state highlighted by our previous QM/MM(FQ) study was found not to be a stable stationary point on the MP2 surface, collapsing instead to a species 0.5 kcal/mol above t′, and differing from t′ only in having a trans orientation of the non-hydrogen-bonded water protons, as opposed to cis in t′. The interior configuration was found to be 1.2 kcal/mol (B3LYP) or 1.4 kcal/mol (MP2) higher in energy than t′, and the surface state 2.2 kcal/mol (B3LYP) or 1.6 kcal/mol (MP2) higher.

We here apply our revised fluctuating charge model to the i, s, t and t′ structures, reporting binding energies in Table 6 and optimal geometries in Table 7. We indeed find that the t state is lower in energy than the interior and surface states, as previously observed. The preference of t over i, however, has diminished from 0.5 to 0.3 kcal/mol. In disagreement with the ab initio results, rather than being 0.6 kcal/mol lower in energy than t, the t′ state is predicted to be 0.8 kcal/mol less favorable. From a consideration of the geometries and charge distribution of the complexes (Figure 1, Table 7), it is not immediately obvious as to the origin of this underestimated stability of t′. As with the i and s structures, the trends in geometry relative to the B3LYP calculations are reasonably reproduced by the QM/MM(FQ) potential. Interestingly, using the QM/MM(FQ) model, we observe a tightening of the H···F bond by about 0.06−0.08 Å with the transition of a water molecule from the first (i and s) to the second solvation shell (t and t′). This effect is 0.09−0.17 Å in the B3LYP calculations and reflects the differing water coordination patterns around the fluoride ion. The largest structural discrepancy in the hybrid model relative to the full quantum mechanical calculation is in the H···F length formed by the fourth water of t and t′ (Table 7). This is the water that does not hydrogen bond to the second solvation shell in t. The H···F distance is increased by 0.19 Å in t′ upon interaction with the second shell water, but increases only by 0.07 Å in the QM/MM(FQ) calculation. Furthermore, the associated trends in the dipole moments of the four waters in t′ relative to t are not observed by the QM/MM(FQ) model. Most conspicuous is the overestimation of the decrease in dipole moment of the fourth water of 0.16 D, whereas the B3LYP calculation predicts a decrease of only 0.04 D. Coupled to this is a large increase of 0.14 D in the B3LYP dipole moment of the second shell water molecule, whereas essentially there is no difference in dipole between t and t′ in the QM/MM(FQ) calculation. The combination of these two factors appears to be responsible for the underestimated stability of t′, and underlines a lack of sensitivity in the polarizable point charge model. Increasing the number of sites and considering out of plane polarization would possibly ameloriate this deficiency.

3.3 Molecular Dynamics. Having examined the structural properties of the cluster at absolute zero, previous studies have amply demonstrated the necessity for inclusion of dynamical effects to fully understand the complex behavior of this system. Two simulations were conducted (see section 2.3), one within the microcanonical (NVE) ensemble and a second with the atomic motion thermostated to room temperature. The experimental enthalpy of solvation for the cluster is −71.7 kcal/mol by combining the $n = 1$ enthalpy of Ashadi et al. with the $n = 2-4$ measurements of Hiraoka et al. However, we may also use our calculated $n = 1$ enthalpy of −27.7 kcal/mol to yield a binding enthalpy for $F(H_2O)_4^-$ of −76.1 kcal/mol. The latter value is in good agreement with our 300 K simulation, from which we obtain an enthalpy of −74.9 kcal/mol (Table 8). The average potential energy of the NVE simulation was found to be −76.1 kcal/mol. However, it is the cluster structure rather than the binding energies which involve the subtlety and are the focus of the dynamical investigation. To discuss the relative proportions of the various structures (Figure 1) along the calculated trajectories, a structure factor, Q, is defined (eq 1). For optimized structures i, s, t′, and t, the corresponding Q values are 0.66, 0.02, 0.65, and 0.29, respectively. The distributions of Q for the NVE and 300 K simulations are given in Figure 3. Predominantly interior states appear to be sampled in the NVE simulation, with Q clustered around 0.7. This was the result found by the MC study of Vaughn et al.,[15] although their study was performed within the isobaric−isothermal ensemble. The fairly tight distribution around the interior state is due in part to the cool temperature ($\langle T \rangle = 96.1$ K). Indeed, to explore the effect of initial geometry, a 20 ps microcanonical simulation was initiated from the t state ($\langle T \rangle = 125.5$ K). This geometry, with the external water molecule hydrogen bonded to two

TABLE 7: Properties of $F(H_2O)_4^-$ Clusters in Interior (i), Surface (s), and Trisolvated (t, t′) Structures Determined at B3LYP/6-311++G(3d,2p) and QM/MM(FQ) Levels[a]

state	model	R_{FH}				μ_{water}			
i	QM/MM(FQ)	1.74	1.75	1.75	1.76	2.63	2.61	2.62	2.60
i	B3LYP	1.72	1.72	1.71	1.66	2.47	2.46	2.47	2.41
s	QM/MM(FQ)	1.76	1.76	1.76	1.76	2.58	2.59	2.58	2.59
s	B3LYP	1.72	1.72	1.72	1.72	2.46	2.46	2.46	2.47
t	QM/MM(FQ)	3.51	1.69	1.69	1.72	2.49	2.93	2.89	2.72
t	B3LYP	3.28	1.63	1.56	1.55	2.38	2.56	2.51	2.46
t′	QM/MM(FQ)	3.28	1.68	1.68	1.79	2.50	2.93	2.92	2.56
t′	B3LYP	3.07	1.55	1.56	1.74	2.52	2.64	2.66	2.42

[a] Fluoride−water hydrogen bond lengths are in Å. For second shell waters, the average fluoride−hydrogen lengths are reported. Dipoles are in debyes.

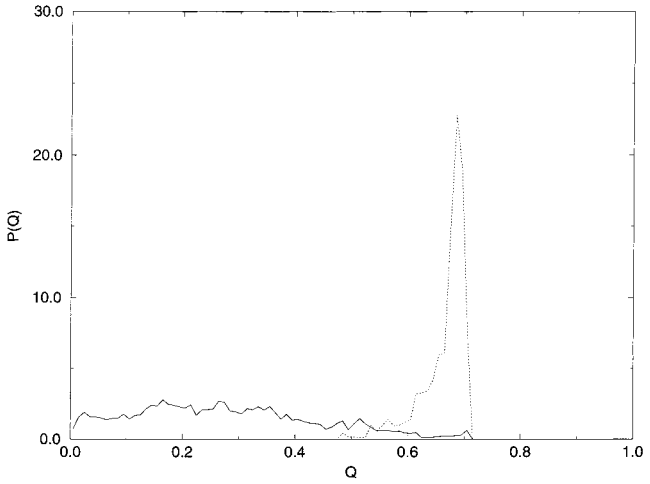

Figure 3. Order parameter distribution, $P(Q)$, calculated during NVE (dashed line) and NVT (solid line) simulations of $F(H_2O)_4^-$.

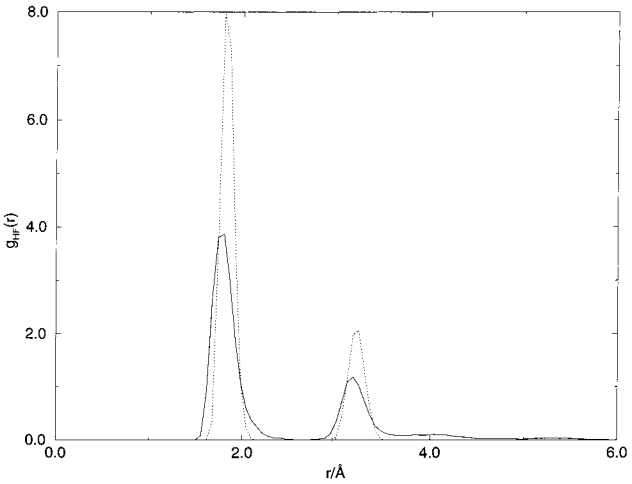

Figure 4. Radial distribution function of water hydrogens about the fluoride ion: NVE (dashed line) and NVT (solid line) simulations.

oxygens of the first shell waters, persisted for 4 ps before one of the water−water bonds was severed. However, for the entire 20 ps, a trisolvate structure was observed, suggesting a barrier between cluster coordinations which could not be surmounted at these low temperatures. In contrast to the NVE trajectories and the previous room temperature ab initio MC study, the 300 K NVT simulation finds a broad distribution of Q between 0.0 and 0.7, indicating the presence of all four structures considered. However, the bulk of the distribution is concentrated between a Q of 0.0 and 0.4, suggesting proportionately less t′ and i states relative to t and s. To subsequently distinguish between t′ and i structures, for which Q is similar, visual inspection identified the fraction of structures lying over the interval $0.64 < Q < 1.00$ to be almost exclusively consisting of interior configurations. The effect of temperature can further be seen in the H···F radial distribution function (Figure 4), where the highly ordered NVE structure is smoothed out by higher temperature, with the appearance of a finite probability of observing water protons out to 5.5 Å, diagnostic of second shell solvation of the fluoride. Direct examination of the trajectory reveals essentially trisolvate-like configurations, with less surface-like structures. The second shell water molecule mainly hydrogen bonds to a single first shell water. This is in accord with our previous simulation, although with the now augmented fluoride/water and weakened intersolvent forces, a larger proportion of tetracoordinate geometries are observed here. A transition is observed at about 16 ps, as evidenced by the shift in O···F bond lengths (Figure 5). The conformational change is between trisolvate-like states, with the interchange of the second shell water molecule. By inspection, the transition is seen to occur via short-lived interior and surface configurations, which persist for about 2 ps.

Therefore, from this model study, we may conclude that t, s, and i states coexist, with a predominance of the trisolvate species. It appears that at lower temperatures, there is insufficient kinetic energy to overcome barriers between 3- and 4-coordinate structures. However, at 300 K, the cluster can readily sample a range of tri- and tetrasolvate geometries.

TABLE 8: Binding Enthalpies of $F(H_2O)_4^-$ Clusters (kcal/mol)

	$\Delta H^{298\ K}$	ref
NVT	−74.9	this work
QM/MM(FQ)	−66.0	13
MM	−80.2	9
experiment	−67.1	10
experiment	−71.7	11

4. Discussion

We have considered in this study the microsolvation of the fluoride anion by a small number of waters. High-level ab initio

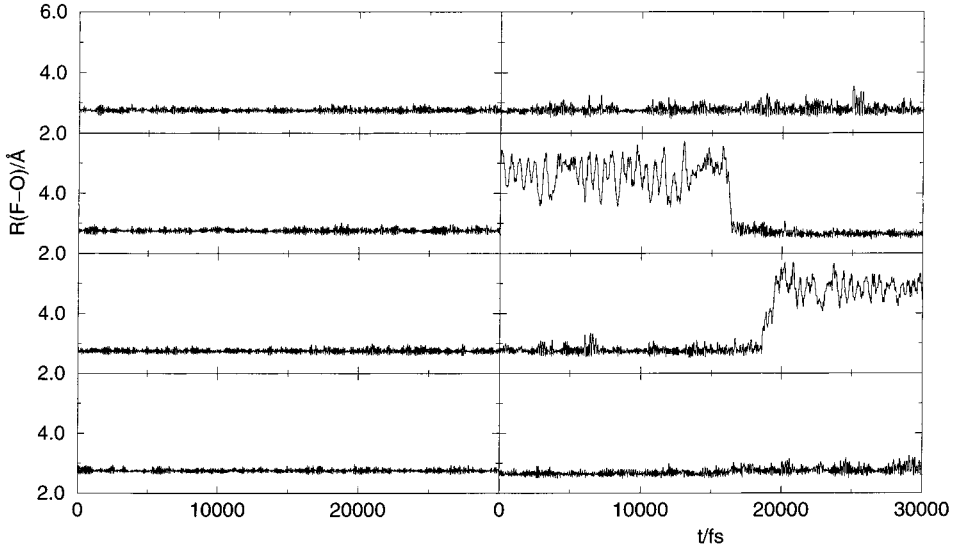

Figure 5. Fluctuation in O···F distance during NVE (left) and NVT (right) simulations of $F(H_2O)_4^-$.

calculations find the binding energy of $F(H_2O)^-$ has converged to a value of −27.3 kcal/mol. However, the variation in the H···F and H−O distances at all levels of theory shows the delicate balance determining this proton position and is a clear reflection of the sensitivity of the structure to the choice of potential. In light of the computationally intensive nature of these potentials, we have endeavored to extrapolate our study to the room temperature behavior of $F(H_2O)_4^-$ clusters by using a hybrid QM/MM model incorporating classical polarizable waters, and basing our parametrization upon high-level ab initio studies of $F(H_2O)^-$ and $(H_2O)_2$. Relative to MP2/6-311++G-(3d,2p) calculations,[15] the energetic trends are reproduced by the QM/MM(FQ) model, with the exception of the t′ geometry, which is not found to be the lowest energy minimum using our hybrid potential. Simulation at room temperature yields an enthalpy of binding in reasonable agreement with experiment. The trajectory explored a range of different structures corresponding to previously identified minima. Trisolvate states were observed to predominate, in which second shell solvation of the anion occurs, with only some sampling of interior and surface states. This finding is in fact converse to the results from the MC study at 300 K, which employed a MP2/6-311++G(3d,2p) description of $F(H_2O)_4^-$, where principally interior states were observed, with only trace amounts of tricoordinate geometries present. We also note the corroboration of this result by a very recent spectroscopic and theoretical study of small fluoride/water clusters by Cabarcos et al.[41] Although the QM/MM(FQ) simulation does identify the existence of both tri- and tetrasolvate geometries at room temperature, evidence would suggest that further development of the form of the potential may be required. Additionally, given the expense of the potential required to model this cluster, the dynamics of the system was followed for only a short period of time. A more complete exploration of phase space would be desirable. Finally, microcanonical simulations at low temperature appeared to explore only a local minimum, whereas room temperature simulation explored a variety of configurations, suggesting energetic barriers of the order of a kilocalorie.

Acknowledgment. We thank EPSRC and Glaxo Wellcome for support. We also thank Prof. T. Martinez, Dr. A. Masters, and Dr. N. Malcolm for helpful discussions.

Supporting Information Available: Tables listing calculated ionization energy of F^-, calculated structure and vibrational frequencies of water, and optimized geometries (5 pages). This material is available free of charge via the Internet at http://pubs.acs.org.

References and Notes

(1) Brown, M. G.; Keutsch, F. N.; Saykally, R. J. *J. Chem. Phys.* **1998**, *109*, 9645.
(2) Gregory, J. K.; Clary, D. C.; Liu, K.; Brown, M. G.; Saykally, R. J. *Science* **1997**, *275*, 814.
(3) Clary, D. C. *J. Chem. Phys.* **1996**, *105*, 6626.
(4) Wales, D. *J. Chem. Phys.* **1997**, *106*, 7193.
(5) Mruzik, M. R.; Abraham, F. F.; Schreiber, D. E. *J. Chem. Phys.* **1976**, *64*, 481.
(6) Perera, L.; Berkowitz, M. L. *J. Chem. Phys.* **1994**, *100*, 3085.
(7) Sremaniak, L. S.; Perera, L.; Berkowitz, M. L. *J. Phys. Chem.* **1996**, *100*, 1350.
(8) Dang, L. X. *J. Chem. Phys.* **1992**, *96*, 6970.
(9) Xantheas, S. S.; Dang, L. X. *J. Phys. Chem.* **1996**, *100*, 3989.
(10) Ashadi, M.; Yamdagni, R.; Kebarle, P. *J. Phys. Chem.* **1970**, *74*, 1475.
(11) Hiraoka, K.; Mizuse, S.; Yamabe, S. *J. Phys. Chem.* **1988**, *92*, 3943.
(12) Xantheas, S. S.; Dunning, T. H. *J. Phys. Chem.* **1994**, *98*, 13489.
(13) Bryce, R. A.; Vincent, M. A.; Malcolm, N. O.; Hillier, I. H.; Burton, N. A. *J. Chem. Phys.* **1998**, *109*, 3077.
(14) Rick, S. W.; Stuart, S. J.; Berne, B. J. *J. Chem. Phys.* **1994**, *101*, 6141.
(15) Vaughn, S. J.; Akhmatskaya, E. V.; Vincent, M. A.; Masters, A. J.; Hillier, I. H. *J. Chem. Phys.* **1999**, *110*, 4338.
(16) Feller, D. *J. Chem. Phys.* **1992**, *96*, 6104.
(17) Schütz, M.; Brdarski, S.; Widmark, P.; Lindh, R.; Karlström, G. *J. Chem. Phys.* **1997**, *107*, 4597.
(18) van Duijneveldt-van de Rijdt, J. G. C. M.; van Duijneveldt, F. B. *J. Chem. Phys.* **1992**, *97*, 5019.
(19) Saebø, S.; Tong, W.; Pulay, P. *J. Chem. Phys.* **1993**, *98*, 2170.
(20) Xantheas, S. S. *J. Chem. Phys.* **1996**, *104*, 8821.
(21) Dunning, T. H. *J. Chem. Phys.* **1989**, *90*, 1007.
(22) Kendall, R. A.; Dunning, T. H.; Harrison, R. J. *J. Chem. Phys.* **1992**, *96*, 6796.
(23) Møller, C.; Plesset, M. S. *Phys. Rev.* **1934**, *46*, 618.
(24) Pople, J. A.; Head-Gordon, M.; Raghavachari, K. *J. Chem. Phys.* **1987**, *87*, 5968.
(25) Becke, A. D. *J. Chem. Phys.* **1993**, *98*, 5648.
(26) *Gaussian 94*, Rev D1; Frisch, M. J.; Trucks, G. W.; Schlegel, H. B.; Gill, P. M. W.; Johnson, B. G.; Robb, M. A.; Cheeseman, J. R.; Keith, T. A.; Petersson, G. A.; Montgomery, J. A.; Raghavachari, K.; Al-Laham, M. A.; Zakrzewski, V. G.; Ortiz, J. V.; Foresman, J. B.; Cioslowski, J.; Stefanov, B. B.; Nanayakkara, A.; Challacombe, M.; Peng, C. Y.; Ayala, P. Y.; Chen, W.; Wong, M. W.; Andres, J. L.; Replogle, E. S.; Gomberts, R.; Martin, R. L.; Fox, D. J.; Binkley, J. S.; Defrees, D. J.; Baker, J.; Stewart, J. P.; Head-Gordon, M.; Gonzalez, C.; Pople, J. A. Gaussian, Inc.: Pittsburgh, PA, 1995.
(27) Stone, A. J. *Chem. Phys. Lett.* **1981**, *83*, 233.
(28) Harrison, M. J.; Burton, N. A.; Hillier, I. H. *J. Am. Chem. Soc.* **1997**, *119*, 12285.
(29) Bryce, R. A.; Buesnel, R.; Masters, A. J.; Hillier, I. H. *Chem. Phys. Lett.* **1997**, *279*, 367.
(30) Swope, W. C.; Andersen, H. C.; Berens, P. H.; Wilson, K. R. *J. Chem. Phys.* **1982**, *76*, 637.
(31) Andersen, H. C. *J. Comput. Phys.* **1983**, *52*, 24.
(32) Nosé, S. *Mol. Phys.* **1984**, *52*, 255.
(33) Hoover, W. G. *Phys. Rev.* **1985**, *A31*, 1695.
(34) Yates, B. F.; Schaefer, H. F.; Lee, T. J.; Rice, J. E. *J. Am. Chem. Soc.* **1988**, *110*, 6327.
(35) Janoschek, R. *Mol. Phys.* **1996**, *89*, 1301.
(36) Combariza, J. E.; Kestner, N. R. *J. Phys. Chem.* **1994**, *98*, 3513.
(37) Odutola, J. A.; Dyke, T. R. *J. Chem. Phys.* **1980**, *72*, 5062.
(38) Curtiss, L. A.; Frurip, D. J.; Blander, M. *J. Chem. Phys.* **1979**, *71*, 2703.
(39) Reimers, J.; Watts, R.; Klein, M. *Chem. Phys.* **1982**, *64*, 95.
(40) Åstrand, P.; Ruud, K.; Mikkelsen, K. V.; Helgaker, T. *J. Phys. Chem. A* **1998**, *102*, 7686.
(41) Cabarcos, O. M.; Weinheimer, C. J.; Lisy, J. M.; Xantheas, S. S. *J. Chem. Phys.* **1999**, *110*, 5.